

CLASTIC MECHANICS

M. D. BOLTON and G. R. McDOWELL
Cambridge University Engineering Department
Trumpington Street, Cambridge, CB2 1PZ, U.K.

Abstract

A study has been made of the micro mechanical origins of hardening in aggregates which comprise elastic-brittle grains. We consider the compression of an aggregate of uniform grains and explain hardening at very small strains in terms of elastic contacts between particles. In the discipline of soil mechanics the terms "yielding" and "plastic hardening" are used to describe the post-elastic behaviour of granular media. Here we propose mechanisms of "clastic yielding" which is the onset of fracture of the weakest particles in the aggregate, followed by "clastic hardening", whereby particles split probabilistically depending on the applied macroscopic stress and the coordination number and size of each particle. This results in the development of a fractal geometry, and the subsequent unload-reload behaviour of such a material will be strongly affected by the disparity in sizes of neighbouring particles.

1. Introduction

Figure 1(a) shows a plot of voids ratio e (volume of voids per unit volume of solids) against mean effective stress p' for a typical compression test on soil. Fig. 1(b) shows the same data with pressure plotted on a logarithmic scale. Engineers interpret regions 1, 2 and 3 as "elastic stiffening", "yielding" and "plastic hardening" respectively. The plastic hardening curve in Fig. 1(b) is remarkably linear: from the earliest publications in soil mechanics, it has been accepted that the isotropic plastic compression of granular media satisfies an approximately linear relationship between voids ratio e and the logarithm of effective macroscopic pressure p' . This linearity applies to a wide range of granular materials (Novello and Johnston, 1989). Engineers describe the behaviour in Fig. 1 by writing:

$$e = f(p') \quad (1)$$

or for the case of plastic compression (region 3)

$$e = e_o - \lambda \ln p' \quad (2)$$

Equations (1) and (2) are dimensionally incorrect: clearly p' should be normalized by a parameter X ,

$$e = f(p'/X) \quad (3)$$

where X has dimensions of stress, and must, for objectivity relate to the soil particles themselves.

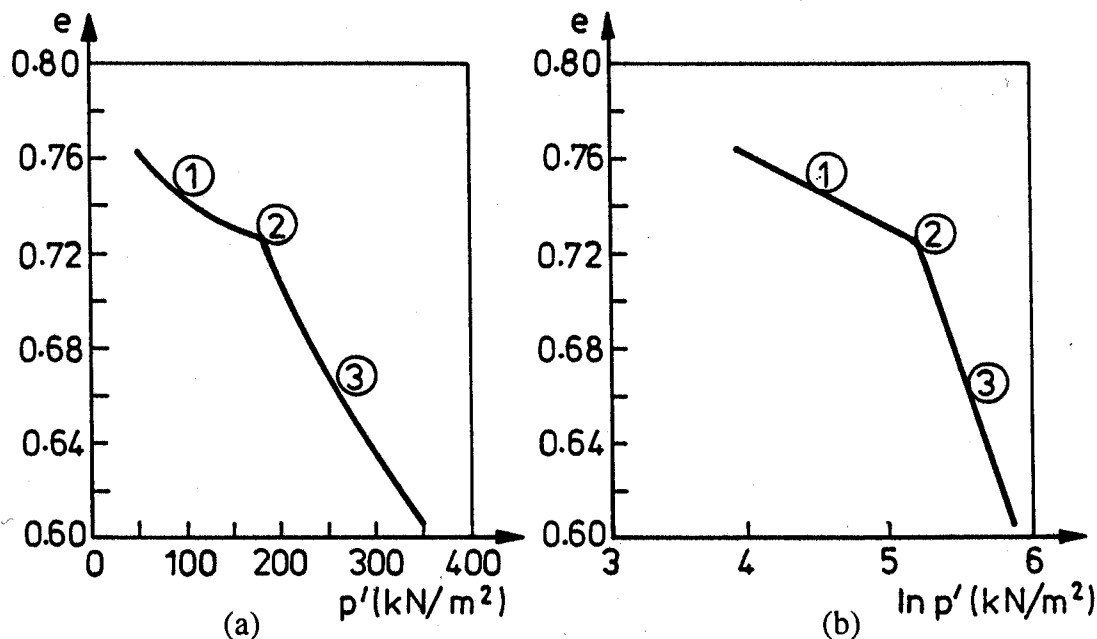


Figure 1. Typical compression curves.

2. Elastic stiffening

At very small strains (less than about 10^{-5}), an aggregate of soil particles behaves entirely elastically. This behaviour must originate solely from the elastic behaviour of individual particle contacts. In this case it is clear that the parameter X in (3) should be an elastic modulus of the particle material. It is found that at very small strains, neglecting changes of voids ratio, the elastic shear modulus of a soil aggregate increases with confining pressure p as $p^{1/2}$ (Hardin and Black, 1966, 1968; Viggiani and Atkinson, 1995). We therefore write:

$$G_o \propto p^{1/2} G_p^{1/2} \quad (4)$$

where G_o is the very small strain shear modulus of soil, and G_p is the elastic shear modulus of the particle material. For isotropic soil with constant Poisson's ratio, the bulk and shear moduli are proportional to one another, so that the bulk modulus has

the same form of pressure dependence. We now examine the micro mechanical origins of the $p^{1/2}$ dependence.

We first consider a mean-field estimate for the stress-strain response of a random array of identical spheres under isotropic compression, following Jenkins and Strack (1993). For an array of particles with an initially isotropic distribution of Hertzian contacts, the bulk modulus of the aggregate, K_v is given by:

$$K_v \propto p^{1/3} G_p^{2/3} C^{2/3} \quad (5)$$

where C is co-ordination number (number of contacts with neighbours). An apparent discrepancy exists between the power of p found to influence stiffness empirically (4) and that developed in mean field theory (5). Goddard (1990) develops two possible explanations. First, the co-ordination number may be a function of mean stress. He analysed a mechanism in which sample-spanning particle chains buckle under compression, until sufficient lateral force is provided by the formation of new contacts. He showed that small rotations at particle contacts increase the average co-ordination number C such that

$$C \propto \varepsilon_v^{1/2} \quad (6)$$

Substituting (6) in (5), it is readily seen that the aggregate elastic modulus then increases with the square root of the confining pressure.

Secondly, he analysed the contact between a plane and a sphere with an obtuse conical asperity, and deduced that for an aggregate of particles with very shallow conical contacts and a fixed co-ordination number, the bulk modulus of the aggregate would be related to the confining pressure by:

$$K_v \propto p^{1/2} G_p^{1/2} \quad (7)$$

Either, or both, of these mechanisms may be involved in raising the power of p which is found empirically to influence the small-strain stiffness of soils.

3. Clastic yielding

For particles of a specified material and of a given size, there is a statistical variation in strength (Moroto and Ishii, 1990). This statistical variation is inherent in the strength of ceramics (Ashby and Jones, 1986). For a sample of uniform grains under compression, the sudden decrease in the rate of hardening which is evident in region 2 of Fig. 1, must be due to the fracture of the weakest particles in the aggregate. We call this "clastic yielding". In this case the parameter X in (3) should relate to the tensile strength of a particle. Lee (1992) measured the tensile strengths of particles by loading grains diametrically between flat platens. When a spherical grain is loaded

diametrically under a pair of forces F , the characteristic tensile stress induced within it can be defined as

$$\sigma = \frac{F}{d^2} \quad (8)$$

Lee used this to calculate the tensile stress at fracture as

$$\sigma_f = \frac{F_f}{d^2} \quad (9)$$

where fracture is interpreted as "particle splitting". We therefore write $X = \sigma_f$ for irrecoverable strains in region 2 of Fig. 1.

4. Evolution of an aggregate

The crushing strength of a particle is a function of its size as a consequence of the statistical variation in the strength of ceramics. Furthermore, if a particle has a high co-ordination number, the load on it is well distributed and the probability of fracture is much lower than that at low co-ordination numbers. In addition, particles are more likely to crush as the stress on a sample of granular material increases. We now use these three criteria to model the evolution of an aggregate of elastic-clastic grains for the simple case of one-dimensional compression.

4.1 A SIMPLE NUMERICAL MODEL

In order to establish a demonstration of the principles involved, a highly simplified two-dimensional numerical model was developed (McDowell, Bolton and Robertson, 1996). The initial sample of material in the model comprises uniformly sized grains, which appear as an array of 50 identical isosceles triangles (Fig. 2(a)). Each particle (triangle) can then split into two identical self-similar triangles, and so on. The triangular laminae used in the model are intended to represent real soil particles, in rather the same way that Palmer and Sanderson (1991) used a hierarchy of splitting cubes to model the crushing of ice. The grains are allowed to split with a probability which increases with the applied macroscopic compressive stress σ and reduces with either an increase in the co-ordination number C or a reduction in particle size d (Weibull, 1951). The model does not deal with local equilibrium or kinematics, but simply with the probability of splitting of grains.

The survival probability $P_s(d)$ for a particle of size d was calculated as:

$$P_s(d) = \exp \left\{ - \left(\frac{d}{d_o} \right)^2 \frac{(\sigma/\sigma_{t,o})^m}{(C-2)^a} \right\} \quad (10)$$

The Weibull modulus m is a measure of the uniformity of the material, and $\sigma_{t,o}$ is a characteristic tensile strength of a particle of size d_o . The factor a can be used to vary the degree to which the co-ordination number C affects the probability of fracture, and may be related to particle angularity.

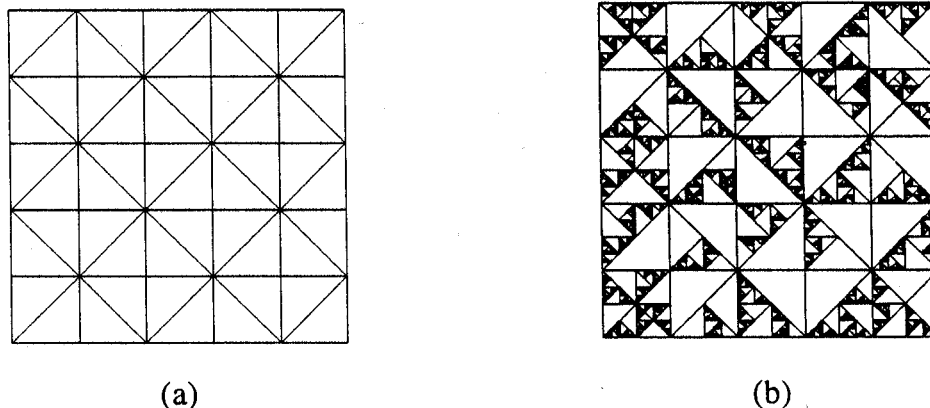


Figure 2. Initial and fractured array of triangles.

For normalisation of the behaviour, the tensile strength $\sigma_{t,o}$ of the initial triangles was set at unity. The initial value of σ was chosen so that only one triangle is likely to break. The stress was then successively incremented and particles were selected for fracture according to (10).

Fig. 3(a) shows the particle size distribution which evolves from taking $m=5$ which fits statistical data, and using $a=5$ which guarantees that co-ordination number is a dominant factor. Fig. 3(b) shows the variation of uniformity coefficient U with increasing macroscopic stress ($U=d_{60}/d_{10}$, where d_{60} is the particle size which 60% by mass of particles are finer than) and Fig. 2(b) shows the resulting array of broken triangles.

4.2 EMERGENCE OF FRACTALS

Fig. 3(a) shows that the curve which evolves of percentage by "mass" (i.e. "area" in the 2-D simulation) of particles smaller than d , versus d on a logarithmic scale is an exponential, which implies a fractal geometry. For a fractal distribution in two dimensions, the percentage by mass of particles smaller than size d , $M(L < d)$ is given by:

$$M(L < d) \propto d^{2-D} \quad (11)$$

D is the fractal dimension, and usually has a value between 2 and 3 for granular materials (Turcotte, 1986). For a corresponding 2-D simulation, the fractal dimension should lie between 1 and 2. For $m=5$ and $a=5$, D was calculated to be 1.36. Only the smaller particles are fracturing each time the applied stress σ is incremented, because

the high co-ordination numbers of the larger particles give them low probabilities of fracture. As the final particle size distribution is approached, the uniformity coefficient approaches a constant value as shown in Fig. 3(b). The form of the curves in Fig. 3(a) is consistent with data for one-dimensionally compressed Ottawa sand (Fig. 4).

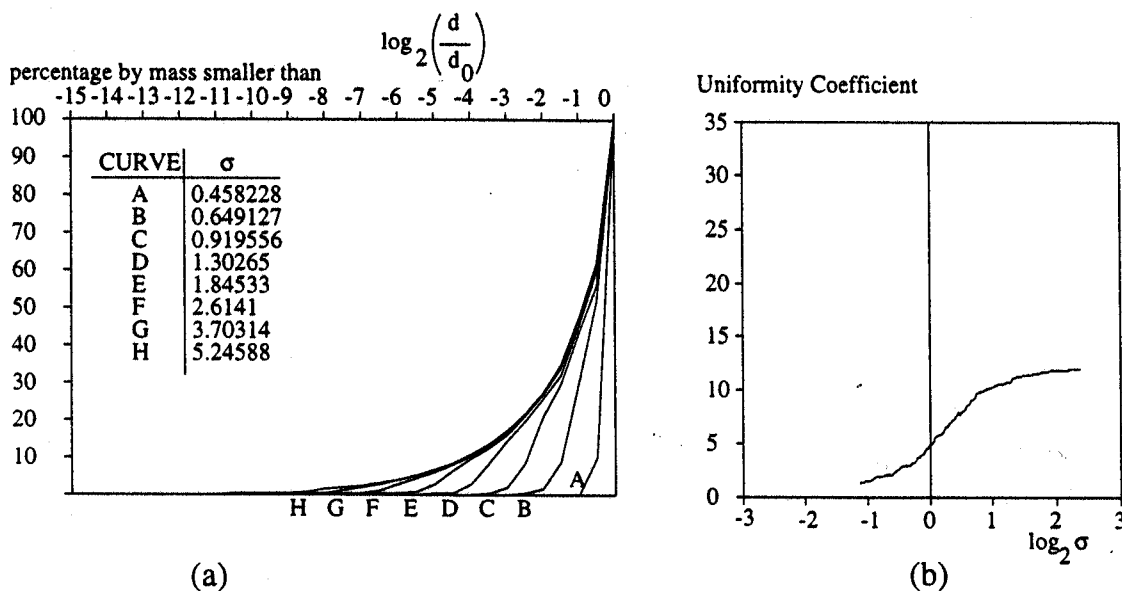


Figure 3. Evolving particle size distributions and uniformity coefficient.

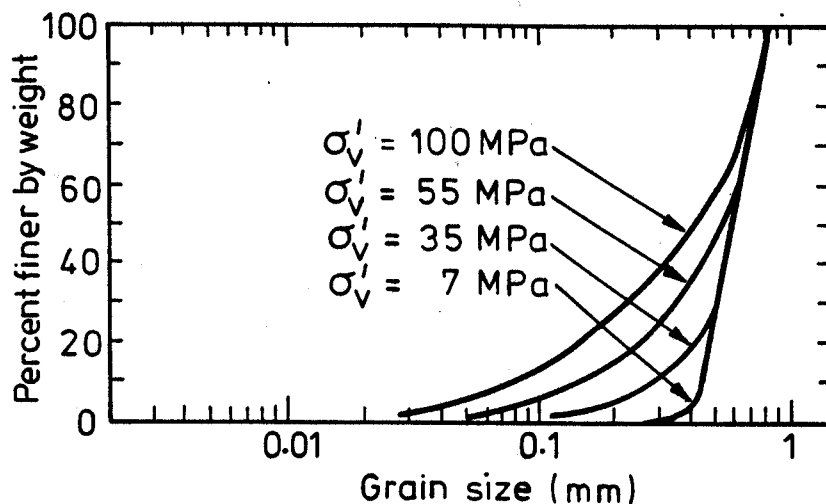


Figure 4. Evolving particle size distributions for Ottawa sand (Fukumoto, 1992).

As with Palmer and Sanderson's fractal model, the range of particle sizes increases with applied stress. The probability of fracture f for the smallest particles of size d_s must be the same each time they fracture. Consequently, Palmer's fractal probability of fracture f can be related to Weibull's survival probability in (10) for the 2-D crushing of triangles:

$$1 - f = P_s = \exp \left\{ - \left(\frac{d_s}{d_o} \right)^2 \frac{(\sigma/\sigma_{t,o})^m}{(C-2)^a} \right\} \quad (12)$$

so that

$$\frac{d_s^2 \sigma^m}{d_o^2 \sigma_{t,o}^m} = \text{constant} \quad (13)$$

A repetition of numerical simulations using different Weibull moduli m , confirmed that equation (13) holds (McDowell, Bolton and Robertson, 1996).

5. Clastic hardening

It is now shown that the evolution of a distribution of particle sizes with constant uniformity coefficient is consistent with the form of the plastic compression curve in region 3 of Fig. 1(b).

5.1 A NEW WORK EQUATION

We modify a work equation proposed by Roscoe, Schofield and Thurairajah (1963) and Schofield and Wroth (1968) to include energy dissipated in fracture and get:

$$q \delta \epsilon_q^p + p' \delta \epsilon_v^p = M p' \delta \epsilon_q^p + \frac{\Gamma dS}{V_s(1+e)} \quad (14)$$

The left hand side represents the work done per unit volume by deviatoric stress q and mean effective stress p' (with corresponding irrecoverable strain increments $\delta \epsilon_q^p$, $\delta \epsilon_v^p$). The first term on the right hand side was identified as internal frictional dissipation, and the new term is the energy dissipated in the creation of new surface area dS for a volume V_s of solids distributed in a gross volume of $V_s(1+e)$ and Γ is the "surface energy". For the case of one-dimensional compression, we decompose the compression of voids ratio δe into elastic and plastic components δe^e and δe^p , following Schofield and Wroth (1968) who showed that if stress is monotonically increased from σ to $\sigma+d\sigma$, $\log \sigma$ increases by $d\sigma/\sigma$ and the plastic component of reduction in voids ratio is given by:

$$d e^p = \Lambda d\sigma/\sigma \quad (15)$$

where Λ is expressed in terms of Schofield and Wroth's parameters λ and κ by $\Lambda = \lambda - \kappa$. We will shortly derive the conditions necessary for Λ to be a constant. Equation (14) gives for the case of uniaxial compression,

$$d e^p = - \frac{\Gamma dS}{(1-\mu)\sigma V_s} \quad (16)$$

where μ is solely a function of the angle of friction ϕ . The form of (16) is consistent with available triaxial data for decomposed granite soil (Miura and O-Hara, 1979).

5.2 POWER LAW COMPRESSION

Equation (16) was used in the numerical model to calculate the hypothetical reduction in voids ratio as the smallest particles fracture with increasing macroscopic stress. Fig. 5 shows the resulting plot for $m=5$, $a=5$. It is evident that an approximately linear-log compression curve develops. This is due to the formation of a fractal geometry. Equation (11) can be used to calculate the total sectional surface area for all the particles in the 2-D sample:

$$S(L > d_s) \propto d_s^{1-D} \quad (17)$$

Substituting (13) and (17) into (16) gives the plastic reduction in voids ratio with applied stress increment $d\sigma$:

$$de^p = -\Lambda \sigma^{\frac{m}{2}(D-1)-1} \frac{d\sigma}{\sigma} \quad (18)$$

In the particular case

$$D = 1 + 2/m \quad (19)$$

equation (18) reduces to equation (15) and can be integrated to give an equation similar in form to (2). In three dimensions (19) becomes

$$D = 2 + 3/m \quad (20)$$

For most soils, m will be between 5 and 10; D is often around 2.5 (Turcotte, 1986; Palmer and Sanderson, 1991), and these values fit (20) rather well. It is therefore proposed that the difference in linearity between normal compression curves for various soils of equal fractal dimension is due to the difference in the variability of the tensile strengths of the particles themselves.

It is now evident that the development of linear-log plastic compression lines in soils has a sound basis in the evolution of a fractal distribution of particle sizes and a constant uniformity coefficient. This is consistent with data for petroleum coke (Biarez and Hicher, 1994, Fig. 6).

5.3 PLASTIC COMPRESSION INDEX Λ AND COMPRESSION INDEX λ

McDowell, Bolton and Robertson (1996) showed that the value of Λ in (18) has the right order of magnitude, comparing with available data for sands and clays. Schofield and Wroth's elastic parameter κ can be added to the plastic compression index Λ to give the compression index λ . Clearly, κ will be a function of the nature of

particle-particle contacts (Hertzian, conical), but the precise micro mechanical origins of κ are not explored here.

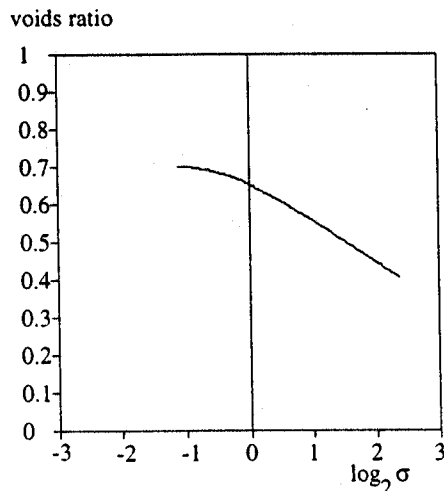


Figure 5. Compression curve for $m=5$, $a=5$.

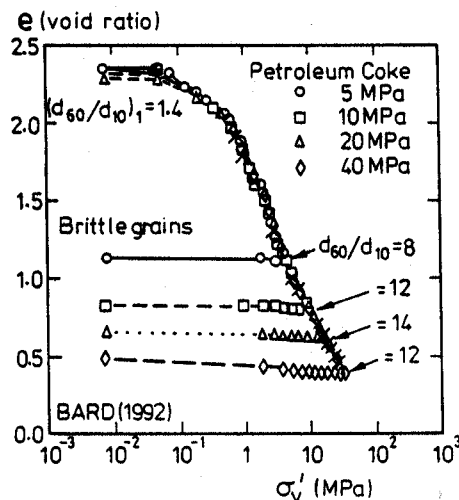


Figure 6. Typical e - $\log \sigma$ plot for petroleum coke.

6. The evolution of soils

If the successive fracture of grains is accepted as the mechanism for clastic (plastic) hardening of soils, particle size disparity must be a hidden feature of all constitutive behaviour. Fig. 7 depicts the qualitative evolution of a soil aggregate in terms of changes of voids ratio with mean effective stress.

A suspended sediment O may be deposited under water as an aggregate of soil particles A. Sands may have been sorted by river and ocean currents and deposited as a uniform aggregate under still water at a relatively low voids ratio. Clay platelets are sub-micron in size and electrically active, settling so slowly that they can agglomerate to form porous macro-particles, here simply called grains, before they finally aggregate as a sediment with a very high voids ratio. Point A in Fig. 7 can represent either grains of sand with internal flaws, or grains of clay composed of electrically bonded platelets. The soil sediment at A may be described as a "genus", from which other soils evolve by cycles of burial and erosion.

As effective stress increases to point B, some grains fracture so that the soil at B will be seen to be a different "species". The broken pieces pack more efficiently, and the voids ratio at B is irrecoverably reduced. Between B and C many grains fracture, and many of the broken fragments fracture again. After the successive fracture of some grains, the size distribution approaches a fractal for the first time at point C. Although soil species D evolves to have more fines than species C, each now approximates to a given fractal geometry which persists as the stress increases.

At D the effective stress may be taken through an unloading-reloading cycle E, F, G, H. This cycle will be conducted on the same soil species, since little extra damage will occur until stresses exceed their previous maximum. As the pre-consolidation pressure is exceeded at H, the states of fractal evolution on the normal consolidation line are resumed, to point I. However, the smallest fragments will eventually reach their comminution limit so that the larger grains split for preference even though they have more neighbours. The accumulation of unbreakable fines would lead to the curvature at point J in Fig. 7. Mixtures of grain types can be considered in the same way. The more crushable grain type would tend to control the compression of the mixture, until those grains reached their comminution limit. This would explain the observation that the compressibility of a clay-sand mixture is simply proportional to the clay fraction.

Soils at points such as B in Fig. 7 are observed to creep, to G for example. This behaviour can be modelled by allowing the tensile strength of particles in (10) to be time-dependent. This time-dependence of strength in oxide ceramics arises from the slow propagation of micro-cracks due to the chemical interaction with water in the environment. This one-parameter addition creates realistic rate effects linked to the popular concept of "apparent pre-consolidation pressure". The species after creep to G is the same as after load cycling to G, and the pre-consolidation pressure is D in either case.

7. Behaviour of a soil species

The transition from recoverable to irrecoverable behaviour (point H in Fig. 7) would be characterised in stress space by a "yield surface". Constitutive models derived from conventional plasticity theory usually invoke the concept of "isotropic hardening" which expands the yield surface homologously as the voids are irrecoverably compressed (e.g. Cam Clay, Schofield and Wroth, 1968). Our view is that the process of isotropic (or anisotropic) hardening occurs by the successive fracture of grains and is better termed "clastic hardening" which follows "clastic yielding".

The behaviour of "over-consolidated soil" at points D, E, F, G, H which would be "inside the yield surface" can be shown not simply to be non-linear elastic, but to involve "kinematic yielding" of a soil species, which seems more appropriate than the previous term "kinematic hardening". Fig. 8 outlines the consequences of a disparity of particle sizes for the deformation of a species such as D. A hypothetical unit cell is considered to contain a rigid kernel, representing a large grain surrounded by a fractal matrix of finer particles. Initial small-strain behaviour will be elastic, albeit inhomogeneous. The lack of strain within the kernel eventually induces a zone of kinematic yielding (particle sliding against particle) in the surrounding matrix, leading to a partial loss of shear stiffness while some normal contact stiffness remains.

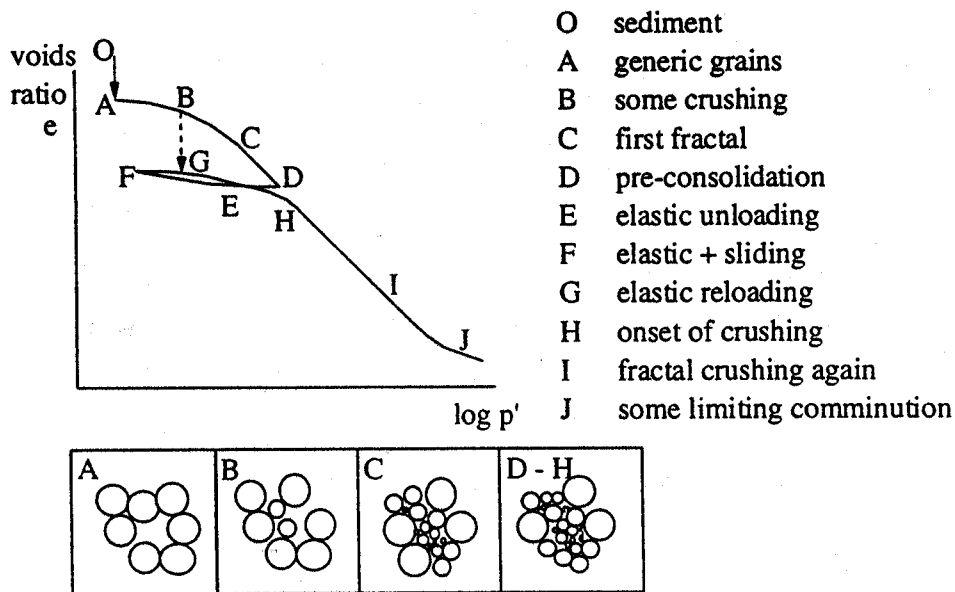


Figure 7. Evolution of soil species.

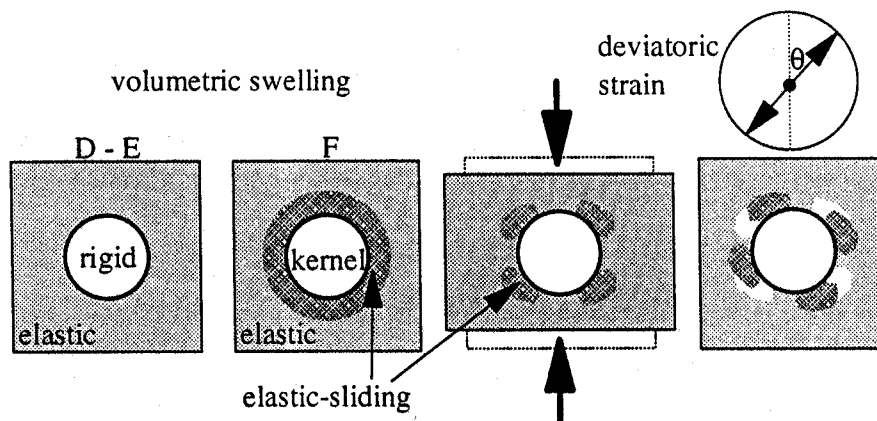


Figure 8. Kinematic yielding within a kernel cell.

From D to E the volumetric expansion will cause the kernel to lose radial stress. At E slip will commence in the matrix at the kernel boundary, due to the local mobilisation of the internal angle of friction between the fine grains. This will successively affect a larger annulus as the boundary stress reduces further, to point F. On re-imposition of spherical compression at F the regime of inter-particle slipping is immediately suspended, since the motion is reversed. The behaviour is elastic on re-loading in the matrix through G but the inhomogeneous stresses may induce clastic yielding "early" so that H falls below D in Fig. 7. This system can provide realistic hysteresis loops such as DEFGH featuring shake-down on cyclic loading, offering compaction if the pores are drained or partial liquefaction if volume is constrained to be constant.

Deviatoric strain starts elastic but eventually induces slip between the matrix and the kernel, on patches which are parallel to planes of maximum shear in the matrix.

Reversal of deviatoric strain re-imposes elastic conditions throughout. Rotation of principal stress direction causes the slip patches to migrate round the kernel, rather in the fashion of a carpet-layer "walking out" ridges, offering realistic progressive strain.

8. Conclusions

The successive fracture of grains under stress has been shown to lead to a fractal grain size distribution using an extension of Weibull statistics. Fractals explain the self-similarity of soils on the normal compression line which is a line of elastic hardening. Elastic yielding is distinguished from kinematic yielding which occurs for a soil species with invulnerable grains, and which is caused by a disparity in particle sizes. The rich gamut of overconsolidated soil behaviour can be reproduced in a kernel cell which induces matrix slip in addition to non-linear elastic deformation, due to the strain discontinuity at the matrix/kernel boundary.

9. References

- Ashby, M.F. and Jones, D.R.H. (1986) *Engineering Materials 2*, Pergamon Press, Oxford.
- Biarez, J. and Hicher, P. (1994) *Elementary Mechanics of Soil Behaviour*, A.A. Balkema, Rotterdam.
- Fukumoto, T. (1992) Particle breakage characteristics in granular soils, *Soils and Foundations* **32**, No. 1, 26-40.
- Goddard, J.D. (1990) Nonlinear elasticity and pressure-dependent wave speeds in granular media, *Proc. R. Soc. Lond. A* **430**, 105-131.
- Hardin, B.O. and Black, W.L. (1966) Sand stiffness under various triaxial stresses, *Journal of the Soil Mechanics and Foundations Division*, ASCE **92**, No. SM2, 27-42.
- Hardin, B.O. and Black, W.L. (1968) Vibration modulus of normally consolidated clay, *Journal of the Soil Mechanics and Foundations Division*, ASCE **94**, No. SM2, 353-369.
- Jenkins, J.T. and Strack, O.D.L. (1992) Mean field inelastic behaviour of random arrays of identical spheres, *Mechanics of Materials* **16**, 25-33.
- Lee, D.M. (1992) *The angles of friction of granular fills*, Ph. D. dissertation, Cambridge University.
- McDowell, G.R., Bolton, M.D. and Robertson, D. (1996) The fractal crushing of granular materials, *J. Mech. Phys. Solids* **44**, No. 12, 2079-2102.
- Miura, N. and O-Hara, S. (1979) Particle-crushing of a decomposed granite soil under shear stresses, *Soils and Foundations* **19**, No. 3, 1-14.
- Moroto, N. and Ishii, T. (1990) Shear strength of uni-sized gravels under triaxial compression, *Soils and Foundations* **30**, No. 2, 23-32.
- Novello, E.A. and Johnston, I.W. (1989) Normally consolidated behaviour of geotechnical materials, *Proc. 12th Int. Conf. Soil Mech., Rio de Janeiro* **3**, 2095-2100.
- Palmer, A.C. and Sanderson, T.J.O. (1991) Fractal crushing of ice and brittle solids, *Proc. R. Soc. Lond. A* **433**, 469-477.
- Roscoe, K.H., Schofield, A.N. and Thurairajah, A. (1963) Yield of clays in states wetter than critical, *Geotechnique* **13**, 211-240.
- Schofield, A.N. and Wroth, C.P. (1968) *Critical State Soil Mechanics*, McGraw-Hill, London.
- Turcotte, D.L. (1986) Fractals and Fragmentation, *Journal of Geophysical Research* **91**, 1921-1926.
- Viggiani, G. and Atkinson, J.H. (1995) Stiffness of fine-grained soils at very small strains, *Geotechnique* **45**, No. 2, 249-265.
- Weibull, W. (1951) A statistical distribution of wide applicability, *J. Appl. Mech.* **18**, 293-297.